## Original Article

# AlphaPPIweb: an integration platform for protein-protein interaction prediction and evaluation

Yen-Yi Liu<sup>1\*</sup>, Chi-Ching Lee<sup>2,3,4\*</sup>, Pei-Hsuan Li<sup>2</sup>, Sung-Huan Yu<sup>11,12</sup>, Mien-Chie Hung<sup>5,6,7,8,9</sup>, Hsin-Mien Hsu<sup>7</sup>, Chih-Chao Yang<sup>10</sup>, Chen-Chieh Huang<sup>10</sup>, Pei-Yao Kuo<sup>1</sup>, Yi-Chuan Li<sup>7,10</sup>

<sup>1</sup>Department of Biology, National Changhua University of Education, Changhua, Taiwan; <sup>2</sup>Department of Computer Science and Information Engineering, Chang Gung University, Taoyuan, Taiwan; <sup>3</sup>Molecular Medicine Research Center, Chang Gung University, Taoyuan, Taiwan; <sup>4</sup>Genomic Medicine Core Laboratory, Chang Gung Memorial Hospital, Taoyuan, Taiwan; <sup>5</sup>Research Center for Cancer Biology, China Medical University, Taichung, Taiwan; <sup>6</sup>Graduate Institute of Biomedical Sciences, China Medical University, Taichung, Taiwan; <sup>7</sup>Cancer Biology and Precision Therapeutics Center, China Medical University, Taichung, Taiwan; <sup>8</sup>Center for Molecular Medicine, China Medical University Hospital, Taichung, Taiwan; <sup>9</sup>Institute of Biochemistry and Molecular Biology, China Medical University, Taichung, Taiwan; <sup>10</sup>Department of Biological Science and Technology, China Medical University, Taichung, Taiwan; <sup>11</sup>Institute of Precision Medicine, College of Medicine, National Sun Yat-sen University, Kaohsiung, Taiwan. \*Equal contributors.

Received August 6, 2025; Accepted September 10, 2025; Epub September 15, 2025; Published September 30, 2025

Abstract: The advent of AlphaFold has markedly advanced structural biology by enabling highly accurate predictions of protein structures. This breakthrough has been further extended by AlphaFold-Multimer, which enables the prediction of protein complex structures. However, currently available tools for predictions have limitations, including usage constraints and the need for extensive postprediction analysis to identify interface residues. To address these challenges, we introduce AlphaPPlweb, a comprehensive web-based platform designed to leverage AlphaPulldown, an AlphaFold-Multimer-based tool, for predicting protein complex structures. Users simply input amino acid sequences, after which AlphaPPlweb generates three-dimensional structural predictions, provides confidence scores, and presents results through intuitive visualizations. The platform facilitates the prediction of interactions between a single bait protein and multiple candidate proteins, thus aiding in the identification of potential ligand-receptor interactions. Furthermore, AlphaPPlweb incorporates automated interface residue analysis immediately following structure prediction, streamlining the workflow and providing comprehensive insights into the predicted complexes. This integrated approach significantly enhances the usability of AlphaPPlweb for biomedical studies and educational applications. By democratizing access to advanced structural prediction tools and enabling a comprehensive analysis of protein interactions, AlphaPPlweb promotes extensive exploration and understanding within the biological research community. AlphaPPlweb is accessible at http://alphappiweb.cmu.edu.tw/.

Keywords: AlphaFold, web service, RNase, Receptor Tyrosine Kinase, structural biology

#### Introduction

Protein-protein interactions (PPIs) play ssessential roles in diverse biological processes, including signal transduction, metabolic regulation, and cellular organization [1-3]. Understanding and predicting PPIs is therefore crucial for elucidating cellular mechanisms and identifying potential therapeutic targets [4-7]. While experimental techniques such as yeast two-hybrid assays and affinity purification assays remain

widely used [8-11], they are time-consuming and often fail to capture transient or weak interactions, limiting their comprehensive utility in large-scale studies [12, 13].

Computational methods have significantly enhanced the efficiency and accuracy of PPI predictions, complementing experimental approaches. A major breakthrough in computational biology was the introduction of AlphaFold [14], which dramatically improved the accuracy of

three-dimensional (3D) protein structure predictions from amino acid sequences. Alpha-Fold's success facilitated further methodological advancements, including AlphaFold-Multimer [15], ColabFold [16], AF2-Complex [17], AlphaPulldown [18], and AlphaFold 3 [19] which have enabled highly accurate predictions of protein complex structures. Notably, AlphaFold 3 offers an accessible graphical user interface (GUI), but it primarily focuses on structure prediction without providing comprehensive model evaluation or detailed post-prediction analyses, which are critical for experimental validation.

Among these computational tools, AlphaPulldown is particularly notable for integrating high-accuracy prediction of protein complexes with robust post-prediction analyses, offering users detailed evaluations of predicted interactions. However, AlphaPulldown's command-line interface limits its accessibility, particularly for experimental researchers who may lack computational expertise. To address this limitation, we have developed AlphaPPIweb, an intuitive web server that combines the powerful predictive capabilities of AlphaPulldown with a userfriendly graphical interface. AlphaPPIweb enables experimental biologists to conduct sophisticated structure-based predictions effortlessly and gain comprehensive insights into the quality and reliability of predicted protein interactions through detailed post-prediction evaluation metrics.

To illustrate AlphaPPIweb's practical utility, we demonstrate its functionality using two biologically relevant protein complexes: EphA4-RNase A family [20, 21] and EphA4-ephrin-A5 [22]. These examples underscore the platform's capability to facilitate precise prediction and thorough analysis of PPIs, streamlining subsequent experimental validation steps.

In conclusion, AlphaPPIweb addresses an important gap in current bioinformatics resources by providing a comprehensive, user-friendly platform specifically tailored to experimental researchers. This accessible interface significantly simplifies advanced PPI predictions and evaluations, empowering researchers to efficiently integrate computational predictions into their experimental workflows, ultimately accelerating discoveries in molecular biology and therapeutic development.

#### Implementation

Implementation of the web interface

We employed various programming languages and technologies for developing the frontend system for our website. Specifically, PHP, Apache, Python, and JavaScript were used. PHP functions as a server-side scripting language, generating dynamic webpage content and managing backend database operations. For the database, a file-based storage approach was adopted. Apache provides the foundational services for the web server infrastructure. The frontend of the web page incorporates foundational components such as Bootstrap 5.3.3, DataTables 2.0, and jQuery 3.7.1. Additionally, Python facilitates data integration between the frontend and backend processes, dynamically generating frontend code that is executed by the browser. Structural visualization packages, including JSmol 16.1.47 and PDBe Molstar 3.1.2, are embedded in the frontend web page using JavaScript.

#### Queuing system

In this study, we developed a distributed queuing system using PHP and a file-based approach to managing user-uploaded data. Upon receiving data, the system promptly creates a dedicated working directory for each job where all meta files generated during the computation process are stored. Each working directory also includes a log file that records the entire execution process. When a job is assigned to compute resources, the system documents the graphical processing units (GPUs) and computing nodes used within the respective directories, ensuring that no GPU is simultaneously allocated to other jobs during the computation process. During computation, users are presented with a waiting screen indicating that computation is in progress. Upon completion, the system delivers results to users via web pages, implemented in PHP to provide real-time visualization and immediate access to results.

#### Tool and interface construction

The development of the AlphaPPIweb Web platform represents a notable advancement in protein structure prediction, particularly in the context of complex protein interactions. Designed to simplify the prediction process,

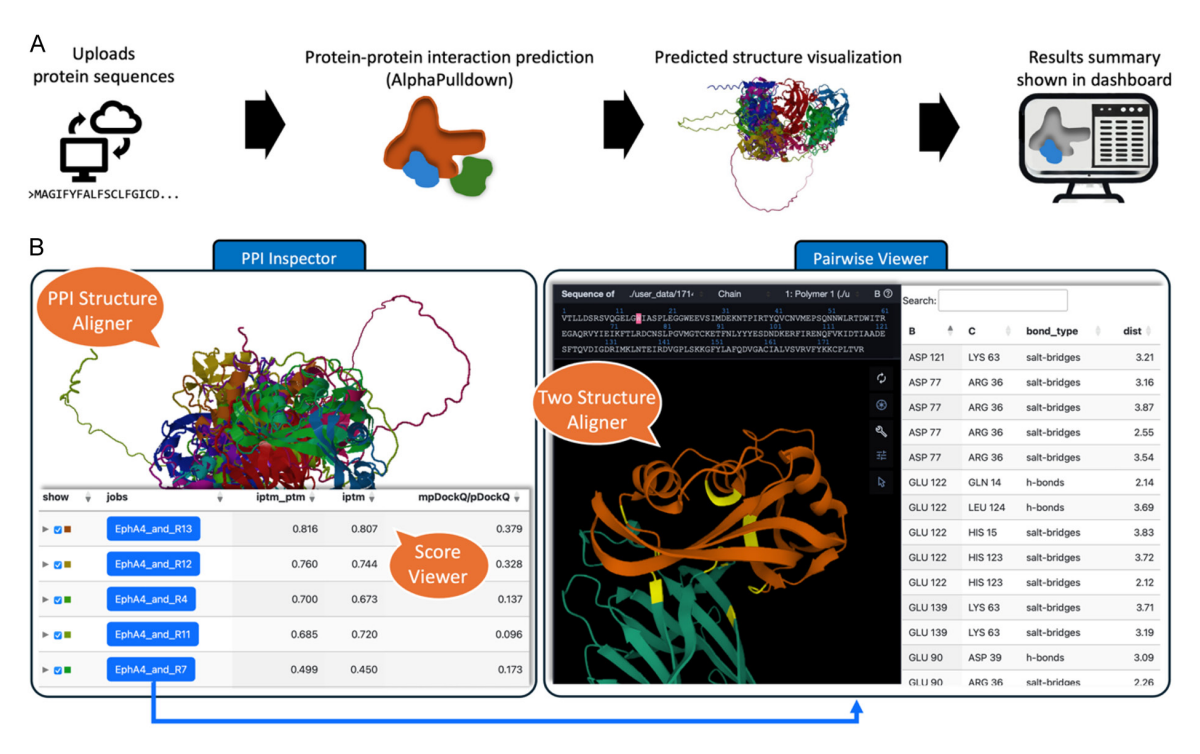


**Figure 1.** Workflow and web interface of AlphaPPIweb. A. The data processing workflow begins with the user uploading the amino acid sequences of the proteins of interest. Once uploaded, the platform's automated pipeline, powered by AlphaPulldown, processes the predictions without requiring any additional configuration or specialized computational resources. The backend AlphaFold service then generates the 3D structures of the proteins, offering researchers a streamlined and efficient method for predicting complex protein interactions. B. The left panel shows 3D structure predictions with confidence scores, presented in an interactive GUI that allows users to rotate, zoom, and manipulate structures, as well as display or hide table columns for detailed analysis. The right panel highlights AlphaPPIweb's key feature - predicting interactions between a single bait protein and multiple candidates, providing insights into protein functions and interactions in complex biological systems.

AlphaPPIweb integrates AlphaPulldown, an AlphaFold-Multimer-based tool, within a highly efficient and user-friendly interface. Researchers can easily use the platform without the need to configure a complex execution environment or establish specialized computational infrastructure. The platform's one-click automated pipeline greatly reduces the manual labor typically associated with protein structure prediction. The workflow begins with the upload of amino acid sequences of interest, after which the platform automatically generates the corresponding 3D protein structures through the backend AlphaFold service. A visual representation of the platform's interface is presented in Figure 1A.

#### Webserver

#### Filtering and visualization

We developed a comprehensive structural alignment and predicted parameter-filtering

interface. As presented in Figure 1B, users can select the results for structural alignment by simply checking checkboxes. The interface allows for simultaneous alignment of multiple structures, facilitating the visualization of relationships between them. Furthermore, the table beneath the alignment section provides various data fields for detailed analysis. As illustrated in Figure 1B, users can dynamically toggle between displaying or hiding certain fields, including polarity scores, hydrophobicity, charge status, and contact pairs, which allows for customization of the viewed data. In addition, scores in the table can be sorted by clicking on the column header, enabling users to filter necessary metric values (Figure 1B, left). To further explore a single structure's sequence and prediction details, users can click the button in the Jobs column of the table shown in Figure 1B. This action opens an interactive 3D molecular visualization module (Figure 1B, right). This module enables users to view and

analyze biomolecular structures and offers multiple viewing modes through a web interface, including space-filling, ball-and-stick, and wireframe models. The interface also includes a sequence-highlighting feature, in which users simply mark a given sequence, and it will be highlighted on the corresponding structure. The table presented in **Figure 1B** displays additional parameters, such as chain ID, types of noncovalent bonds, and distances between bonded atoms. This allows for quick filtering of relevant structural details.

#### Job queuing and execution

Given the increased computational time required for processing longer sequences, which can extend up to several hours, we developed a distributed queuing system to optimize resource allocation. This system is designed to maximize GPU resources by allowing only one user to access a GPU at a time. Other users' calculation tasks are added to a queue and processed sequentially in the order they are submitted. We prioritize user data protection by not permanently storing input or output data. The calculation results are temporarily available via the unique link provided to the user. These results are automatically deleted after a predetermined period to ensure privacy and optimize system resources. After the expiration period, the data is no longer accessible. Once the current computation is completed, the system automatically reallocates resources to the next user in line, minimizing resource contention and maximizing computational efficiency. This approach not only optimizes the distribution of computational resources but also reduces overall waiting times, offering a practical and efficient solution for large-scale protein structure analysis.

#### Example analysis

Predicting EphA4-ephrin-A5 complex models with AlphaPPIweb close to the crystal structure

To demonstrate the capability of AlphaPPIweb in facilitating structural predictions, we utilized our web service and the AlphaFold 3 (AF3) server (https://alphafoldserver.com/) to predict the EphA4-ephrin-A5 complex and compared the predictions with the known crystal structure [22] (PDB ID: 4M4R) (**Figures 2A** and <u>S1</u>). We used ephrin-A5 (UniProt ID: P52803) as the

candidate sequence, and the EphA4 ligand-binding domain (residues 31-209, UniProt ID: P54764) was used as the bait. Upon submission of the files, a project ID was generated, and the web platform automatically refreshed to display the prediction results. Subsequently, we downloaded the predicted structures and the table from the webpage for further analysis.

The root mean square deviation (RMSD) of  $C\alpha$ atoms between the AlphaPPIweb model and the crystal structure was 1.69 Å, whereas the RMSD for the AF3 model was 1.20 Å. These results illustrate the ability of both AlphaPPIweb and AF3 to generate highly accurate structural predictions. The minor RMSD difference of 0.49 Å between the AF3 and AlphaPPIweb models demonstrates that AlphaPPIweb can perform comparably to AF3 in certain cases. Additionally, the interface residues of the EphA4-ephrin-A5 complex in both models were highly conserved relative to the crystal structure (Figure 2B). The G-H loop (residues 118 to 132) of ephrin-A5, responsible for receptor-recognition [23, 24], inserted into the EphA4 binding pocket, exhibited an RMSD of 0.27 Å (15 Ca atoms) between the predicted models and the crystal structure. Both AlphaPPIweb and AF3 correctly placed ephrin-A5 within the conserved ephrin-binding pocket, demonstrating AlphaPPIweb's utility for screening virtual ligandreceptor pairs.

RNase A family-EphA4 complex prediction indicating RNase13 as a potential EphA4 binder

Studies have identified members of the RNase A family as ligands for receptor tyrosine kinases in cancer cells [20, 25-27]. Notably, RNase1 has been characterized as a secretory ligand for EphA4, promoting breast tumor initiation [20, 21]. Given the shared biochemical properties of the RNase A family, such as their positively charged surface regions, we investigated whether other RNase A family proteins could also act as ligands for EphA4, potentially playing roles in initiating other cancer types. For the virtual screening of novel EphA4 ligands in the RNase A family, we used all 13 human RNase A family proteins as candidates and the EphA4 ligand-binding domain (residues 31-209, Uni-Prot ID: P54764) as the bait. Following submission, the process took 9 hours and 14 min-

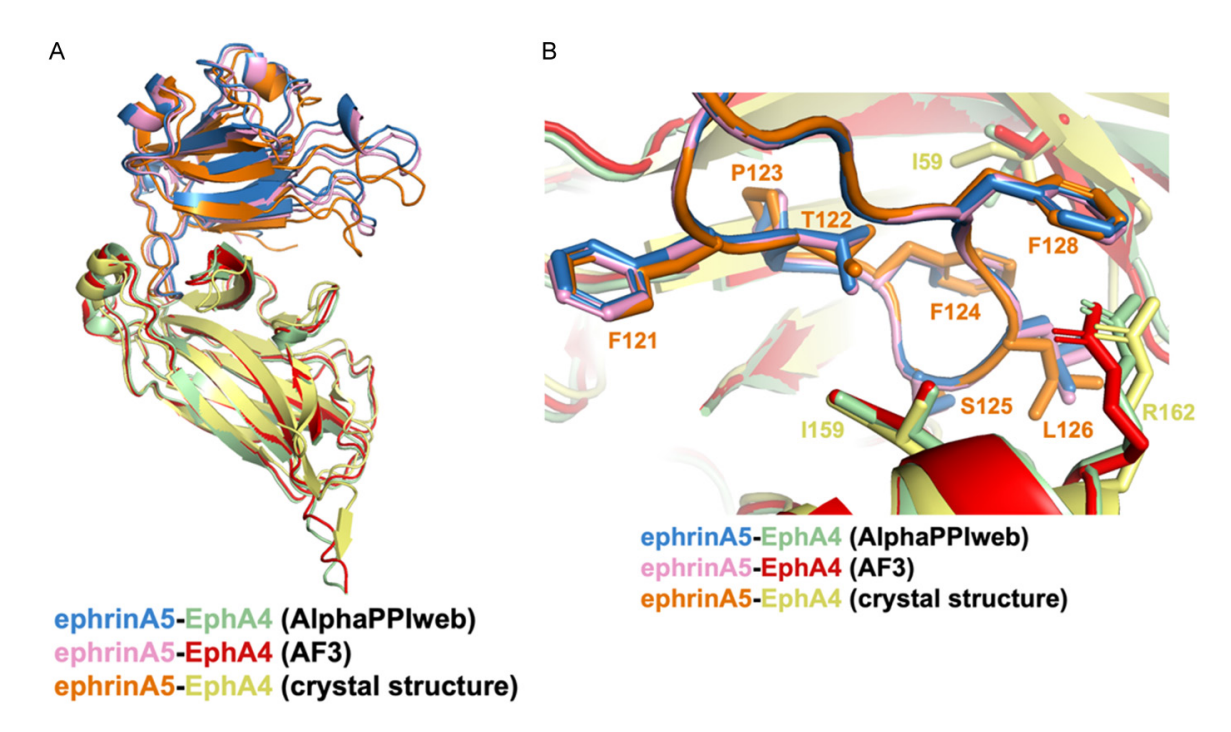


**Figure 2.** AlphaFold models demonstrate high structural conservation with EphA4-ephrin complexes. A. Superimposed AlphaFold models and the crystal structure of the EphA4-ephrin-A5 complex. The complex structure predicted by AlphaPPlweb is colored green for EphA4 and blue for ephrin-A5; the complex structure predicted by AlphaFold 3 is colored red for EphA4 and pink for ephrin-A5. In the crystal structure, EphA4 is denoted by yellow and ephrin-A5 by orange. B. Residues 121-128 of ephrin-A5, depicted in stick representation, bind to the ephrin-binding pocket of EphA4. The ephrin-A5 residues are colored orange, and the EphA4 residues are colored yellow.

utes to complete. All the sequences used in this example are listed in <u>Tables S1</u> and <u>S2</u>, and the results are shown in <u>Figure S2</u>.

The various acronyms and scores in the output table provide detailed information about the predicted protein-protein interactions and their stability. The ipTM (interface Predicted Template Modeling score) evaluates the quality of the predicted interface structure, with higher values indicating greater confidence and accuracy. Values higher than 0.8 indicate confident, high-quality predictions, whereas values below 0.6 suggest a likely failure in prediction. ipTM values ranging from 0.6 to 0.8 fall into a gray zone, where predictions may be either accurate or inaccurate [15]. The mpDockQ (multipleinterface predicted Docking Quality score) and pDockQ (predicted DockQ) assess the reliability of the docking model. A pDockQ score  $\geq 0.23$ indicates acceptable quality [28]. Polar, hydrophobic, and charged values represent the percentage of their respective amino acid types relative to the total number of interface residues. Additional scores include sc (shape complementarity), which represents geometric shape complementarity of protein-protein interfaces, sc ranges between 0 and 1, with sc=1 indicating that two proteins mesh precisely [29]. hb (hydrogen bonding) and sb (salt bridges) represent specific interactions at the interface. The int\_solv\_en (interface solvation energy, kcal/mol) measures the change in solvation energy upon binding [30]; for instance, a value of -5.39 indicates that binding reduces the solvation energy required to maintain the interface, favoring a stable interaction. Together, these AlphaPulldown-based metrics provide a comprehensive understanding of the interaction's quality, specificity, and stability, highlighting the molecular determinants of binding and offering a robust foundation for experimental validation.

Our web server enhances AlphaPulldown with an automated alignment feature that organizes predicted models based on the bait protein, enabling the efficient identification of distinct binding sites. Utilizing these features, the predicted RNase-binding sites were grouped into two clusters based on their competition with ephrin (Figure 3A). Specifically, RNS2, RNS3,

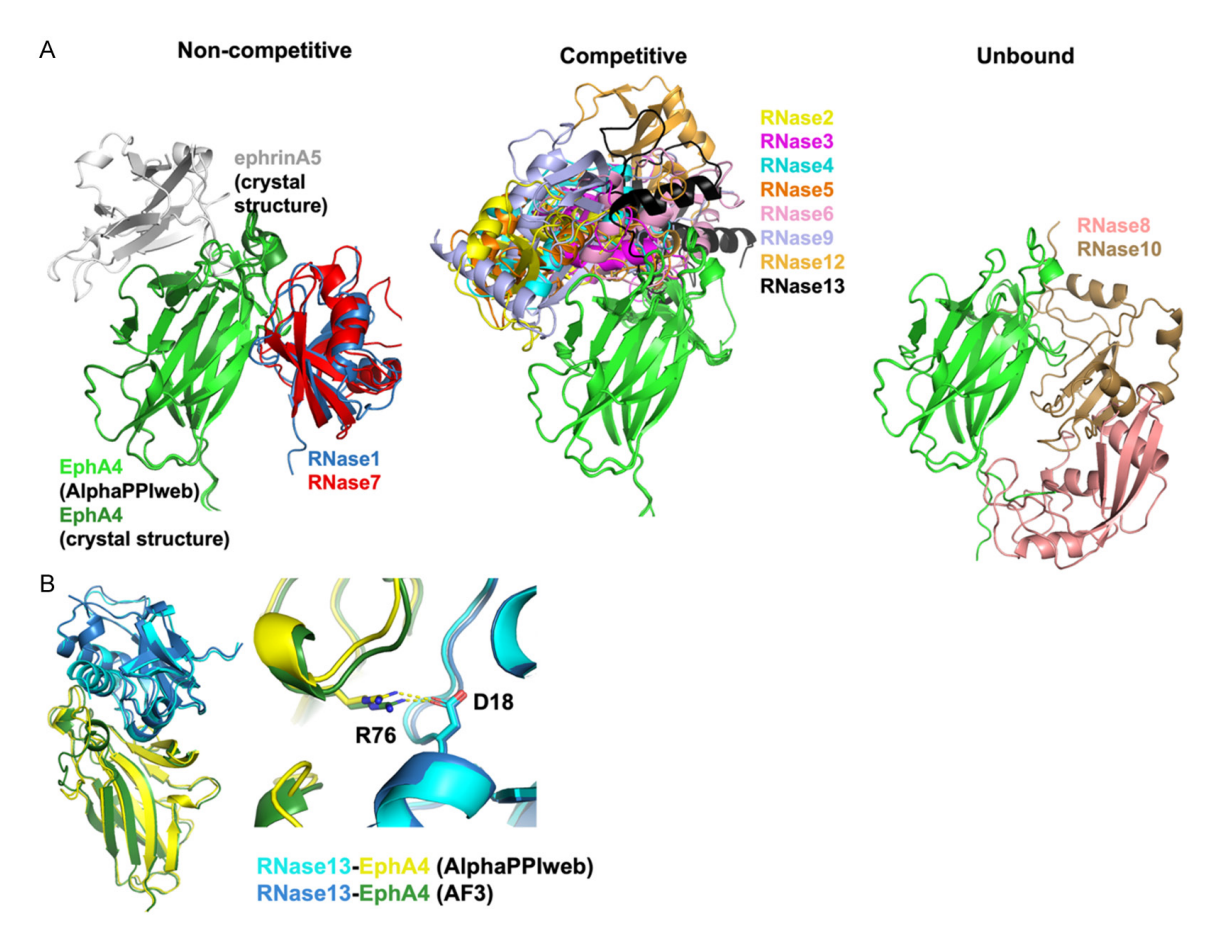


**Figure 3.** RNase A family-EphA4 complex prediction, highlighting RNase13 as a potential EphA4 binder and as a competitive ligand. A. On the basis of the predicted binding positions relative to ephrin-A5 on EphA4, the RNase A family proteins were classified into noncompetitive, competitive, and unbound categories. EphA4 is depicted in green, whereas the RNases are depicted in different colors. B. Superimposed models of the RNase13-EphA4 complex, predicted by AlphaPPlweb and AlphaFold 3 (AF3), reveal a root mean square deviation of only 0.78 Å between the main chains, demonstrating high structural similarity. A common salt bridge is observed at the interface between Asp18 of RNase13 and Arg76 of EphA4.

RNS4, RNS5, RNS6, RNS9, RNS12, and RNS13 were predicted to compete as ligands for ephrin (**Figure 3A**, middle). Conversely, RNS1 and RNS7 were predicted to be noncompeting ligands, sharing the same binding site and maintaining a conserved orientation, suggesting that they possess structural features recognizable by AlphaPPIweb (**Figure 3A**, left). However, RNS8 and RNS10 were predicted to have minimal interactions with EphA4, indicating that they may not act as potential ligands (**Figure 3A**, right).

Notably, the pDockQ score for the EphA4-RNase11 complex is relatively low (0.096), contrasting with the higher ipTM score (0.72) and the energetically favorable int\_solv\_en value (-22.89) (Figure S2). This inconsistency may

arise from AlphaPPIweb predicting a disordered structure for RNase11 within the complex model. The disordered model is not captured by the ipTM score, emphasizing the need to incorporate additional metrics, such as pTM and pDockQ, when assessing predicted models for a more robust evaluation. Different scores provide insight into distinct aspects of the model, making reliance on a single score insufficient. An integrated analysis of multiple scores, supplemented by structural visualization, is critical for drawing reliable conclusions.

Next, we compared the prediction results of AlphaPPIweb with those of AF3. The ipTM scores from the two servers of AlphaFold are listed in **Table 1**. Although the RNase1-EphA4 complex has been reported as a ligand-recep-

**Table 1**. Analysis of potential interactions and binding sites of the RNase A family with EphA4 by comparing predictions from two web services

	AlphaPPIweb model			AF3 model	
	ephrin-binding site	ipTM	pDockQ	ephrin-binding site	ipTM
RNS1	non-competitive	0.34	0.103	competitive	0.14
RNS2	competitive	0.18	0.170	competitive	0.16
RNS3	competitive	0.2	0.162	competitive	0.17
RNS4	competitive	0.67	0.137	competitive	0.16
RNS5	competitive	0.24	0.136	competitive	0.14
RNS6	competitive	0.19	0.240	competitive	0.12
RNS7	non-competitive	0.45	0.173	competitive	0.21
RNS8	unbound	0.23	0.317	competitive	0.26
RNS9	competitive	0.2	0.117	non-competitive	0.15
RNS10	unbound	0.17	0.089	competitive	0.22
RNS11	failed*	0.72	0.096	competitive	0.45
RNS12	competitive	0.74	0.328	competitive	0.15
RNS13	competitive	0.81	0.379	competitive	0.66

<sup>\*</sup>RNS11 was predicted to have a disordered structure when complexed with EphA4 by using AlphaPPIweb. The ipTM (interface Predicted Template Modeling score) measures the quality of a predicted interface structure, with scores above 0.8 indicating high confidence, below 0.6 suggesting likely failure, and 0.6-0.8 representing uncertain predictions. pDockQ (predicted DockQ) assesses the reliability of the docking model. A pDockQ score ≥ 0.23 indicates acceptable quality.

tor relationship, the ipTM scores predicted by the two servers of AlphaFold are both low. Scores below 0.6 may indicate failed prediction models, while scores above 0.8 suggest confident, high-quality predictions. Notably, the models predicted by AlphaPPIweb for EphA4 complexes with RNase1, RNase4, and RNase12 all have higher ipTM scores compared to the AF3 version, suggesting that AlphaPPIweb may be more advantageous in identifying potential binding partners. However, further experimental validation is required to exclude false positives. Surprisingly, both servers of AlphaFold predict RNase13 as a strong potential binder to EphA4, with AlphaPPIweb predicting an ipTM score of 0.81 and AF3 predicting a score of 0.66. In addition to the ipTM score, three other critical metrics support the potential of RNase13 as an EphA4 ligand (Figure S2). The pDockQ score (0.379), the highest among all RNases, indicates a high-quality model. The elevated sc score (0.511) reflects favorable geometric shape complementarity, correlating with interaction energies such as van der Waals forces and non-polar desolvation. Moreover, the int\_solv\_en value (-17.23) signifies a reduction in solvation energy upon complex formation, suggesting an energetically favorable and stable interaction.

When comparing the RNase13-EphA4 complexes predicted by the two AlphaFold servers, we found that their predictions are highly consistent, with an RMSD of 0.78 Å. In both models, a salt bridge between Asp18 of RNase13 and Arg76 of EphA4 was observed (Figure 3B). This consistent prediction indicates that RNase13 is likely to be a ligand for EphA4. At present, research on RNase13 function is very limited. It has been speculated that RNase13 lacks ribonuclease activity, and recent studies in male mice suggest that RNase13 may be related to reproductive aging [31, 32], although the conclusions remain unclear. Overall, the AlphaFold predicted models indicate a high structural compatibility between RNase13 and EphA4, necessitating experimental validation of their ligand-receptor relationship and the elucidation of their physiological significance.

#### Discussion

The 3D structures of protein complexes are essential for understanding molecular interactions, elucidating molecular functions, and driving drug development. However, comprehensively investigating these complexes through experimental methods alone is often resource-intensive and time-consuming, particularly for complex or difficult-to-study target proteins.

Advances in machine learning, such as the development of AlphaFold and other innovative tools, have revolutionized the landscape of protein structure prediction. These innovations have greatly increased the efficiency and accuracy of predicting protein complex structures, underscoring the need for rigorous evaluation methodologies. Common evaluation metrics, such as ipTM, pTM, and mpDockQ/pDockQ scores, along with detailed analyses of interface residues, are now widely used to ensure the reliability of predictions.

The AlphaPPIweb web server is a substantial advancement in this domain. Powered by AlphaPulldown computations, the platform offers researchers a user-friendly interface for predicting interactions among multiple ligandreceptor pairs. AlphaPPIweb not only automates the computation of evaluation scores but also provides comprehensive analyses of protein interface residues. Moreover, the platform's ability to visualize and align all predicted receptor structures enables researchers to identify key interface regions and potential binding sites with precision. We anticipate that AlphaPPIweb will serve as an indispensable tool for researchers engaged in ligand-receptor complex structure prediction. Its applications span academic research, biomedical studies, and educational contexts, thus facilitating the advancement of protein interaction studies and accelerating the pace of drug discovery.

#### Acknowledgements

This study was supported by grants from the National Science and Technology Council of Taiwan (NSTC 113-2221-E-018-016-MY3, NSTC 114-2221-E-182-045, NSTC 114-2320-B-039-063, NSTC 114-2639-B-039-001-ASP, and T-star Center NSTC 114-2634-F-039-001); the Ministry of Health and Welfare Taiwan (MOHW114-TDU-B-222-144016 and MOHW-114-TDU-B-222-000020); and the "Cancer Biology and Precision Therapeutics Center, China Medical University" from The Featured Areas Research Center Program within the framework of the Higher Education Sprout Project by the Ministry of Education (MOE) in Taiwan.

#### Disclosure of conflict of interest

None.

Address correspondence to: Yi-Chuan Li, Department of Biological Science and Technology, China Medical University, Taichung 406040, Taiwan. Tel: +886-4-22053366; E-mail: ycl@mail.cmu.edu.tw

#### References

- [1] Rual JF, Venkatesan K, Hao T, Hirozane-Kishikawa T, Dricot A, Li N, Berriz GF, Gibbons FD, Dreze M, Ayivi-Guedehoussou N, Klitgord N, Simon C, Boxem M, Milstein S, Rosenberg J, Goldberg DS, Zhang LV, Wong SL, Franklin G, Li S, Albala JS, Lim J, Fraughton C, Llamosas E, Cevik S, Bex C, Lamesch P, Sikorski RS, Vandenhaute J, Zoghbi HY, Smolyar A, Bosak S, Sequerra R, Doucette-Stamm L, Cusick ME, Hill DE, Roth FP and Vidal M. Towards a proteome-scale map of the human protein-protein interaction network. Nature 2005; 437: 1173-1178.
- [2] Stelzl U, Worm U, Lalowski M, Haenig C, Brembeck FH, Goehler H, Stroedicke M, Zenkner M, Schoenherr A, Koeppen S, Timm J, Mintzlaff S, Abraham C, Bock N, Kietzmann S, Goedde A, Toksoz E, Droege A, Krobitsch S, Korn B, Birchmeier W, Lehrach H and Wanker EE. A human protein-protein interaction network: a resource for annotating the proteome. Cell 2005; 122: 957-968.
- [3] Kaneda A, Seike T, Danjo T, Nakajima T, Otsubo N, Yamaguchi D, Tsuji Y, Hamaguchi K, Yasunaga M, Nishiya Y, Suzuki M, Saito JI, Yatsunami R, Nakamura S, Sekido Y and Mori K. The novel potent TEAD inhibitor, K-975, inhibits YAP1/TAZ-TEAD protein-protein interactions and exerts an anti-tumor effect on malignant pleural mesothelioma. Am J Cancer Res 2020; 10: 4399-4415.
- [4] Venkataraman S, Li YC, Hung ZW, Hsu YC, Yang Z, Tsai TI, Hung MC, Han KH and Lin CW. Epitope-guided selection of CXCR4-targeting antibodies using AlphaFold3 for GPCR modulation and cancer therapy. Am J Cancer Res 2025; 15: 2127-2139.
- [5] Lee PC, Kumar V, Sivakumar G, Tseng TY, Li YC, Jiang YC, Hsiao YC, Lin HW, Chang CS and Hung MC. Development of triazole-based PKCinhibitors to overcome resistance to EGFR inhibitors in EGFR-mutant lung cancers. Am J Cancer Res 2023; 13: 4693-4707.
- [6] Li Y, Chen L, Feng L, Zhu M, Shen Q, Fang Y, Liu X and Zhang X. NEK2 promotes proliferation, migration and tumor growth of gastric cancer cells via regulating KDM5B/H3K4me3. Am J Cancer Res 2019; 9: 2364-2378.
- [7] Wang HC, Li YC and Hung MC. Itaconate targets the ERK2 signal to suppress estrogen receptor-positive breast cancer cell growth. Am J Cancer Res 2025; 15: 1133-1147.

- [8] Bruckner A, Polge C, Lentze N, Auerbach D and Schlattner U. Yeast two-hybrid, a powerful tool for systems biology. Int J Mol Sci 2009; 10: 2763-2788.
- [9] Miller J and Stagljar I. Using the yeast two-hybrid system to identify interacting proteins. Methods Mol Biol 2004; 261: 247-262.
- [10] Wong JH, Alfatah M, Sin MF, Sim HM, Verma CS, Lane DP and Arumugam P. A yeast two-hybrid system for the screening and characterization of small-molecule inhibitors of proteinprotein interactions identifies a novel putative Mdm2-binding site in p53. BMC Biol 2017; 15: 108.
- [11] Bellanger S, Tan CL, Xue YZ, Teissier S and Thierry F. Tumor suppressor or oncogene? A critical role of the human papillomavirus (HPV) E2 protein in cervical cancer progression. Am J Cancer Res 2011; 1: 373-389.
- [12] Jorgenson LM, Olson-Wood MG and Rucks EA. Shifting proteomes: limitations in using the BioID proximity labeling system to study SNARE protein trafficking during infection with intracellular pathogens. Pathog Dis 2021; 79: ftab039.
- [13] Kim DI, Jensen SC, Noble KA, Kc B, Roux KH, Motamedchaboki K and Roux KJ. An improved smaller biotin ligase for BioID proximity labeling. Mol Biol Cell 2016; 27: 1188-1196.
- [14] Jumper J, Evans R, Pritzel A, Green T, Figurnov M, Ronneberger O, Tunyasuvunakool K, Bates R, Zidek A, Potapenko A, Bridgland A, Meyer C, Kohl SAA, Ballard AJ, Cowie A, Romera-Paredes B, Nikolov S, Jain R, Adler J, Back T, Petersen S, Reiman D, Clancy E, Zielinski M, Steinegger M, Pacholska M, Berghammer T, Bodenstein S, Silver D, Vinyals O, Senior AW, Kavukcuoglu K, Kohli P and Hassabis D. Highly accurate protein structure prediction with AlphaFold. Nature 2021; 596: 583-589.
- [15] Evans R, O'Neill M, Pritzel A, Antropova N, Senior A, Green T, Žídek A, Bates R, Blackwell S, Yim J, Ronneberger O, Bodenstein S, Zielinski M, Bridgland A, Potapenko A, Cowie A, Tunyasuvunakool K, Jain R, Clancy E, Kohli P, Jumper J and Hassabis D. Protein complex prediction with AlphaFold-Multimer. bioRxiv 2022; 2021.2010.2004.463034.
- [16] Mirdita M, Schutze K, Moriwaki Y, Heo L, Ovchinnikov S and Steinegger M. ColabFold: making protein folding accessible to all. Nat Methods 2022; 19: 679-682.
- [17] Gao M, Nakajima An D, Parks JM and Skolnick J. AF2Complex predicts direct physical interactions in multimeric proteins with deep learning. Nat Commun 2022; 13: 1744.
- [18] Yu D, Chojnowski G, Rosenthal M and Kosinski J. AlphaPulldown-a python package for protein-

- protein interaction screens using AlphaFold-Multimer. Bioinformatics 2023; 39: btac749.
- [19] Abramson J, Adler J, Dunger J, Evans R, Green T, Pritzel A, Ronneberger O, Willmore L, Ballard AJ, Bambrick J, Bodenstein SW, Evans DA, Hung CC, O'Neill M, Reiman D, Tunyasuvunakool K, Wu Z, Zemgulyte A, Arvaniti E, Beattie C, Bertolli O, Bridgland A, Cherepanov A, Congreve M, Cowen-Rivers AI, Cowie A, Figurnov M, Fuchs FB, Gladman H, Jain R, Khan YA, Low CMR, Perlin K, Potapenko A, Savy P, Singh S, Stecula A, Thillaisundaram A, Tong C, Yakneen S, Zhong ED, Zielinski M, Zidek A, Bapst V, Kohli P, Jaderberg M, Hassabis D and Jumper JM. Accurate structure prediction of biomolecular interactions with AlphaFold 3. Nature 2024: 630: 493-500.
- [20] Lee HH, Wang YN, Yang WH, Xia W, Wei Y, Chan LC, Wang YH, Jiang Z, Xu S, Yao J, Qiu Y, Hsu YH, Hwang WL, Yan M, Cha JH, Hsu JL, Shen J, Ye Y, Wu X, Hou MF, Tseng LM, Wang SC, Pan MR, Yang CH, Wang YL, Yamaguchi H, Pang D, Hortobagyi GN, Yu D and Hung MC. Human ribonuclease 1 serves as a secretory ligand of ephrin A4 receptor and induces breast tumor initiation. Nat Commun 2021; 12: 2788.
- [21] Li YC, Yamaguchi H, Liu YY, Hsu KC, Sun TH, Sun PC and Hung MC. Structural insights into EphA4 unconventional activation from prediction of the EphA4 and its complex with ribonuclease 1. Am J Cancer Res 2022; 12: 4865-4878.
- [22] Xu K, Tzvetkova-Robev D, Xu Y, Goldgur Y, Chan YP, Himanen JP and Nikolov DB. Insights into Eph receptor tyrosine kinase activation from crystal structures of the EphA4 ectodomain and its complex with ephrin-A5. Proc Natl Acad Sci U S A 2013; 110: 14634-14639.
- [23] Day B, To C, Himanen JP, Smith FM, Nikolov DB, Boyd AW and Lackmann M. Three distinct molecular surfaces in ephrin-A5 are essential for a functional interaction with EphA3. J Biol Chem 2005; 280: 26526-26532.
- [24] Nikolov D, Li C, Lackmann M, Jeffrey P and Himanen J. Crystal structure of the human ephrin-A5 ectodomain. Protein Sci 2007; 16: 996-1000.
- [25] Wang YN, Lee HH, Chou CK, Yang WH, Wei Y, Chen CT, Yao J, Hsu JL, Zhu C, Ying H, Ye Y, Wang WJ, Lim SO, Xia W, Ko HW, Liu X, Liu CG, Wu X, Wang H, Li D, Prakash LR, Katz MH, Kang Y, Kim M, Fleming JB, Fogelman D, Javle M, Maitra A and Hung MC. Angiogenin/ribonuclease 5 is an EGFR ligand and a serum biomarker for erlotinib sensitivity in pancreatic cancer. Cancer Cell 2018; 33: 752-769, e8.
- [26] Wang YN, Lee HH and Hung MC. A novel ligandreceptor relationship between families of ribo-

#### AlphaPPIweb: predicting and scoring PPIs

- nucleases and receptor tyrosine kinases. J Biomed Sci 2018; 25: 83.
- [27] Liu C, Zha Z, Zhou C, Chen Y, Xia W, Wang YN, Lee HH, Yin Y, Yan M, Chang CW, Chan LC, Qiu Y, Li H, Li CW, Hsu JM, Hsu JL, Wang SC, Ren N and Hung MC. Ribonuclease 7-driven activation of ROS1 is a potential therapeutic target in hepatocellular carcinoma. J Hepatol 2021; 74: 907-918.
- [28] Bryant P, Pozzati G and Elofsson A. Improved prediction of protein-protein interactions using AlphaFold2. Nat Commun 2022; 13: 1265.
- [29] Malhotra S, Joseph AP, Thiyagalingam J and Topf M. Assessment of protein-protein interfaces in cryo-EM derived assemblies. Nat Commun 2021; 12: 3399.

- [30] Krissinel E and Henrick K. Inference of macromolecular assemblies from crystalline state. J Mol Biol 2007; 372: 774-797.
- [31] Huang Y, Li X, Sun X, Yao J, Gao F, Wang Z, Hu J, Wang Z, Ouyang B, Tu X, Zou X, Liu W, Lu M, Deng C, Yang Q and Xie Y. Anatomical transcriptome atlas of the male mouse reproductive system during aging. Front Cell Dev Biol 2022; 9: 782824.
- [32] Cho S, Beintema JJ and Zhang J. The ribonuclease A superfamily of mammals and birds: identifying new members and tracing evolutionary histories. Genomics 2005; 85: 208-220.

## AlphaPPIweb: predicting and scoring PPIs

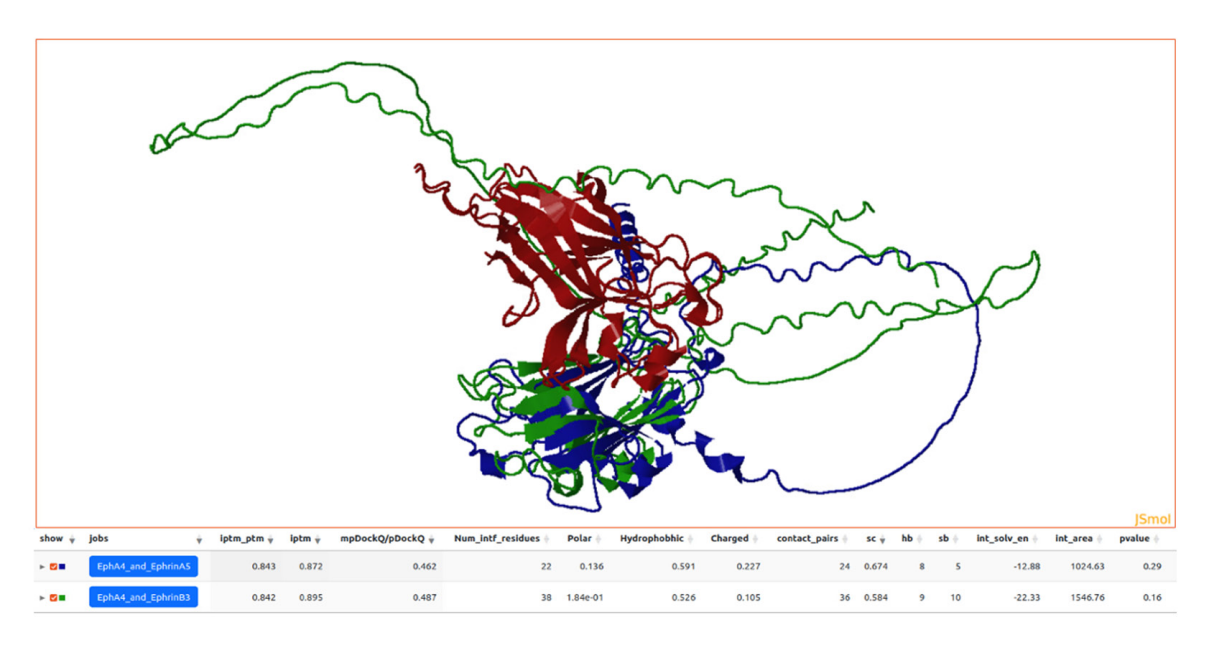


Figure S1. An example of the predicted structure of the EphA4 and ephrin-A5/B3 complex.

### **Table S1.** Input sequences of the EphA4 example

Table 61. Input sequences of the Eph/A+ example		
ephrinA5	MLHVEMLTLVFLVLWMCVFSQDPGSKAVADRYAVYWNSSNPRFQRGDYHIDVCINDYLDVFCPHYEDSVPEDK- TERYVLYMVNFDGYSACDHTSKGFKRWECNRPHSPNGPLKFSEKFQLFTPFSLGFEFRPGREYFYISSAIPDN- GRRSCLKLKVFVRPTNSCMKTIGVHDRVFDVNDKVENSLEPADDTVHESAEPSRGENAAQTPRIPSRLLAILLFL- LAMLLTL	
ephrinB3	MGPPHSGPGGVRVGALLLLGVLGLVSGLSLEPVYWNSANKRFQAEGGYVLYPQIGDRLDLLCPRARPPG-PHSSPNYEFYKLYLVGGAQGRRCEAPPAPNLLLTCDRPDLDLRFTIKFQEYSPNLWGHEFRSHHDYYIIATSDG-TREGLESLQGGVCLTRGMKVLLRVGQSPRGGAVPRKPVSEMPMERDRGAAHSLEPGKENLPGDPTSNATSR-GAEGPLPPPSMPAVAGAAGGLALLLLGVAGAGGAMCWRRRRAKPSESRHPGPGSFGRGGSLGLGGGGGMG-PREAEPGELGIALRGGGAADPPFCPHYEKVSGDYGHPVYIVQDGPPQSPPNIYYKV	
EphA4	VTLLDSRSVQGELGWIASPLEGGWEEVSIMDEKNTPIRTYQVCNVMEPSQNNWLRTDWITREGAQRVYIE-IKFTLRDCNSLPGVMGTCKETFNLYYYESDNDKERFIRENQFVKIDTIAADESFTQVDIGDRIMKLNTEIRDVG-PLSKKGFYLAFQDVGACIALVSVRVFYKKCPLTVR	

## AlphaPPIweb: predicting and scoring PPIs

RNase1	KESRAKKFQRQHMDSDSSPSSSSTYCNQMMRRRNMTQGRCKPVNTFVHEPLVDVQN- VCFQEKVTCKNGQGNCYKSNSSMHITDCRLTNGSRYPNCAYRTSPKERHIIVACEGSPYVPVHFDASVEDST
RNase2	KPPQFTWAQWFETQHINMTSQQCTNAMQVINNYQRRCKNQNTFLLTTFANVVNVCGNPNMTCPSNK- TRKNCHHSGSQVPLIHCNLTTPSPQNISNCRYAQTPANMFYIVACDNRDQRRDPPQYPVVPVHLDRII
RNase3	RPPQFTRAQWFAIQHISLNPPRCTIAMRAINNYRWRCKNQNTFLRTTFANVVNVCGNQSIRCPHNRTLNNCHRSR FRVPLLHCDLINPGAQNISNCTYADRPGRRFYVVACDNRDPRDSPRYPVVPVHLDTTI
RNase4	QDGMYQRFLRQHVHPEETGGSDRYCNLMMQRRKMTLYHCKRFNTFIHEDIWNIRSICSTTNIQCKNGKMN-CHEGVVKVTDCRDTGSSRAPNCRYRAIASTRRVVIACEGNPQVPVHFDG
RNase5	QDNSRYTHFLTQHYDAKPQGRDDRYCESIMRRRGLTSPCKDINTFIHGNKRSIKAICENKNGNPHRENLRISKSSFQVTTCKLHGGSPWPPCQYRATAGFRNVVVACENGLPVHLDQSIFRRP
RNase6	WPKRLTKAHWFEIQHIQPSPLQCNRAMSGINNYTQHCKHQNTFLHDSFQNVAAVCDLLSIVCK- NRRHNCHQSSKPVNMTDCRLTSGKYPQCRYSAAAQYKFFIVACDPPQKSDPPYKLVPVHLDSIL
RNase7	KPKGMTSSQWFKIQHMQPSPQACNSAMKNINKHTKRCKDLNTFLHEPFSSVAATCQTPKIACKNGD- KNCHQSHGAVSLTMCKLTSGKHPNCRYKEKRQNKSYVVACKPPQKKDSQQFHLVPVHLDRVL
RNase8	KPKDMTSSQWFKTQHVQPSPQACNSAMSIINKYTERCKDLNTFLHEPFSSVAITCQTPNIACKNSCKNCHQSH-GPMSLTMGELTSGKYPNCRYKEKHLNTPYIVACDPPQQGDPGYPLVPVHLDKVV
RNase9	QEVDTDFDFPEEDKKEEFEECLEKFFSTGPARPPTKEKVKRRVLIEPGMPLNHIEYCNHEIMGKNVYYKHRW-VAEHYFLLMQYDELQKICYNRFVPCKNGIRKCNRSKGLVEGVYCNLTEAFEIPACKYESLYRKGYVLITC-SWQNEMQKRIPHTINDLVEPPEHRSFLSEDGVFVISP
RNase10	LHMATAVLEESDQPLNEFWSSDSQDKAEATEEGDGTQTTETLVLSNKEVVQPGWPEDPILGEDEVGGNKMLRAS ALFQSNKDYLRLDQTDRECNDMMAHKMKEPSQSCIAQYAFIHEDLNTVKAVCNSPVIACELKGGKCHKSSR-PFDLTLCELSQPDQVTPNCNYLTSVIKKHIIITCNDMKRQLPTGQ
RNase11	EASESTMKIIKEEFTDEEMQYDMAKSGQEKQTIEILMNPILLVKNTSLSMSKDDMSSTLLTFRSLHYNDPKGNSSGNDKECCNDMTVWRKVSEANGSCKWSNNFIRSSTEVMRRVHRAPSCKFVQNPGISCCESLELENTVCQFTT-GKQFPRCQYHSVTSLEKILTVLTGHSLMSWLVCGSKL
RNase12	EAVMSTLEHLHVDYPQNDVPVPARYCNHMIIQRVIREPDHTCKKEHVFIHERPRKINGICISPKKVACQNLSAIF-CFQSETKFKMTVCQLIEGTRYPACRYHYSPTEGFVLVTCDDLRPDSFLGYVK
RNase13	MDIKMQIGSRNFYTLSIDYPRVNYPKGFRGYCNGLMSYMRGKMQNSDCPKIHYVIHAPWKAIQKFCKYSDSFCENYNEYCTLTQDSLPITVCSLSHQQPPTSCYYNSTLTNQKLYLLCSRKYEADPIGIAGLYSGI

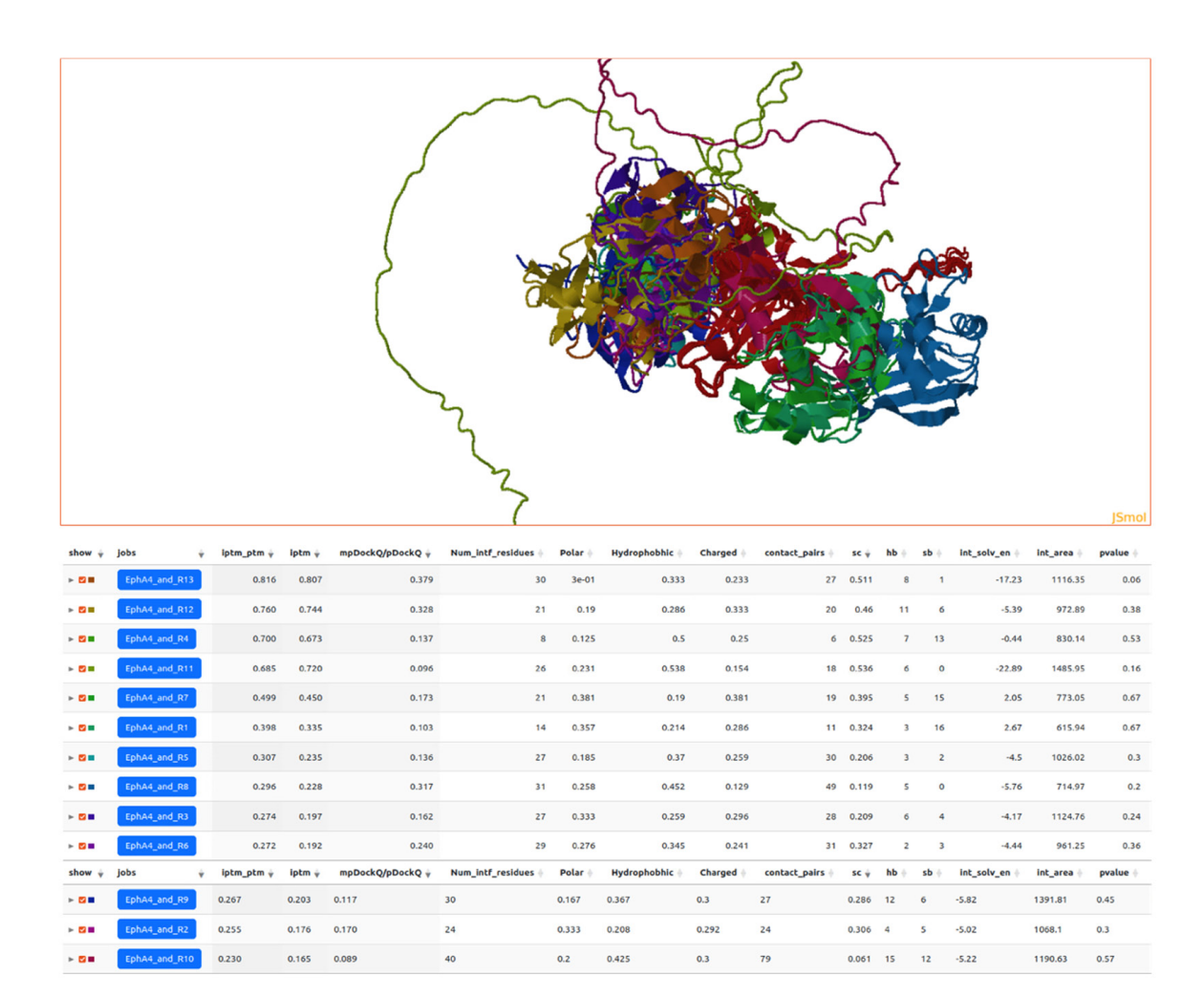


Figure S2. An example of the predicted structure of the EphA4 and RNase A family complex. The table is ordered by the iptm\_ptm score. ipTM (interface Predicted Template Modeling score) evaluates interface quality, with higher scores indicating greater confidence, while pTM (Predicted Template Modeling score) assesses overall model quality. mpDockQ and pDockQ estimate docking quality, with higher values reflecting better predictions. Num\_intf\_residues represents the number of residues involved in the interface. Polar (Ser, Thr, Asn, Gln, His and Tyr), Hydrophobic (Ala, Leu, Ile, Val, Phe, Trp, Cys, Met) and Charged (Asp, Glu, Lys, Arg) quantify specific types of interactions at the interface. contact\_pairs were defined as the number of atomic contacts between the interface residues from the interacting chains. sc represents the geometric shape complementarity of protein-protein interfaces, ranging between 0 and 1, with sc=1 indicating that two proteins mesh precisely. hb and sb measure the number of hydrogen bonds and salt bridges, respectively. int\_solv\_en calculates the energy difference between the bound and unbound monomers caused by the solvation effect, and int\_area represents the total interfacial area. p value measures interface specificity, with P=0.5 indicating an average interface, P>0.5 suggesting less hydrophobicity, and P<0.5 reflecting high hydrophobicity and interaction specificity.